JOURNAL OF BACTERIOLOGY, June 1997, p. 3972–3980 Vol. 179, No. 12
0021-9193/97/$04.00+0

Pathways for Utilization of Carbon Reserves in *Desulfovibrio gigas* under Fermentative and Respiratory Conditions

PAULA FARELEIRA,[1,2] JEAN LEGALL,[1,3] ANTÓNIO V. XAVIER,[1] AND HELENA SANTOS[1]*

Instituto de Tecnologia Química e Biológica, Universidade Nova de Lisboa,[1] and Estação Agronómica Nacional, Instituto Nacional de Investigação Agrária,[2] P-2780 Oeiras, Portugal, and Department of Biochemistry and Molecular Biology, University of Georgia, Athens, Georgia 30602[3]

Received 8 January 1997/Accepted 8 April 1997

The sulfate-reducing bacterium *Desulfovibrio gigas* accumulates large amounts of polyglucose as an endogenous carbon and energy reserve. In the absence of exogenous substrates, the intracellular polysaccharide was utilized, and energy was conserved in the process (H. Santos, P. Fareleira, A. V. Xavier, L. Chen, M.-Y. Liu, and J. LeGall, Biochem. Biophys. Res. Commun. 195:551–557, 1993). When an external electron acceptor was not provided, degradation of polyglucose by cell suspensions of *D. gigas* yielded acetate, glycerol, hydrogen, and ethanol. A detailed investigation of the metabolic pathways involved in the formation of these end products was carried out, based on measurements of the activities of glycolytic enzymes in cell extracts, by either spectrophotometric or nuclear magnetic resonance (NMR) assays. All of the enzyme activities associated with the glycogen cleavage and the Embden-Meyerhof pathway were determined as well as those involved in the formation of glycerol from dihydroxyacetone phosphate (glycerol-3-phosphate dehydrogenase and glycerol phosphatase) and the enzymes that catalyze the reactions leading to the production of ethanol (pyruvate decarboxylase and ethanol dehydrogenase). The key enzymes of the Entner-Doudoroff pathway were not detected. The methylglyoxal bypass was identified as a second glycolytic branch operating simultaneously with the Embden-Meyerhof pathway. The relative contribution of these two pathways for polyglucose degradation was 2:3. ^{13}C-labeling experiments with cell extracts using isotopically enriched glucose and ^{13}C-NMR analysis supported the proposed pathways. The information on the metabolic pathways involved in polyglucose catabolism combined with analyses of the end products formed from polyglucose under fermentative conditions provided some insight into the role of NADH in *D. gigas*. In the presence of electron acceptors, NADH resulting from polyglucose degradation was utilized for the reduction of sulfate, thiosulfate, or nitrite, leading to the formation of acetate as the only carbon end product besides CO_2. Evidence supporting the role of NADH as a source of reducing equivalents for the production of hydrogen is also presented.

A wide range of microorganisms is able to synthesize and store polyglucose or other polymers as intracellular carbon reserves; usually, the accumulation of these compounds occurs as a result of restrictive growth conditions in the presence of an excess source of carbon and energy (7, 30). It has been shown that some sulfate-reducing bacteria, namely, *Desulfobulbus propionicus* and several *Desulfovibrio* species, can accumulate high amounts of polyglucose when the growth medium is depleted of essential nutrients, for example, nitrogen or iron, but *Desulfovibrio gigas* accumulates high levels of polyglucose even under optimal growth conditions (38). Recent studies with *D. gigas* showed that nongrowing cell suspensions could generate NTP from the utilization of the internal storage polymer in both anaerobic and aerobic conditions. These findings demonstrated the remarkable capability of this strict anaerobe to survive under aerobic conditions at the expense of the internal carbon reserves and triggered further interest in the elucidation of the metabolism of polyglucose in this organism (33).

Low-molecular-mass compounds such as lactate, pyruvate, malate, fumarate, ethanol, glycerol, and molecular hydrogen are the most usual substrates for *Desulfovibrio* species, and the pathways involved in their catabolism have been studied extensively in the last decades (10). In contrast, very little is known about the capability of *Desulfovibrio* to utilize sugars as carbon sources for growth or about the reactions involved in the degradation of sugar compounds, e.g., fructose and glucose (25, 43). One of the few exceptions reported to date is *Desulfovibrio fructosovorans*, which is capable of growing on fructose as a sole carbon source (25).

In previous work with *D. gigas*, we detected the formation of acetate, glycerol, and ethanol as major end products of polyglucose metabolism under fermentative conditions and in the absence of any exogenous carbon substrate (33). Surprisingly, the same end products, although in different relative proportions, were formed after treatment of cells with sodium fluoride, a well known inhibitor of enolase. Also, the total amount of carbon products did not decrease, as anticipated, although the intracellular accumulation of 3-phosphoglycerate (33) indicated the expected inhibitory effect of fluoride at the level of enolase. These intriguing results suggested the presence of a second glycolytic pathway, distinct from the Embden-Meyerhof pathway, capable of sustaining an efficient utilization of polyglucose without the participation of enolase. Here we present a detailed search of the enzyme activities and metabolic pathways involved in the degradation of the polyglucose reserve by *D. gigas*: the alternative pathway was identified, and the effect of the availability of electron acceptors on the metabolism of polyglucose was also studied.

* Corresponding author. Mailing address: Instituto de Tecnologia Química e Biológica, Rua da Quinta Grande 6, Apartado 127, P-2780 Oeiras, Portugal. Phone: 351 1 4426171. Fax: 351 1 4428766. E-mail: santos@itqb.unl.pt.

MATERIALS AND METHODS

Abbreviations. APS, adenosine 5′-phosphosulfate; DCPIP, 2,6-dichlorophenol indophenol; MOPS, 3-(*N*-morpholino)propanesulfonic acid; MTT, 3-(4′,5′-dim-

ethylthiazol-2-yl)-2,4-diphenyltetrazolium bromide; NMR, nuclear magnetic resonance; NTP, nucleoside triphosphates; PMS, phenazine methosulfate.

Materials. A Sephadex G-25 column was purchased from Pharmacia Fine Chemicals AB (Uppsala, Sweden). Enzymes and coenzymes for the enzymatic assays were obtained from Boehringer Mannheim GmbH (Mannheim, Germany) or Sigma Chemical Co. (St. Louis, Mo.). Glycogen from rabbit liver was obtained from Sigma. ^{13}C-enriched glucose was purchased from Campro Benelux (Veenendaal, The Netherlands), Omicron Biochemicals (South Bend, Ind.), and Sigma. Dihydroxyacetone phosphate was prepared from the dimethyl ketal di(monocyclohexylammonium) salt according to the instructions of the supplier (Sigma). All other chemicals were of reagent grade.

Growth conditions and preparation of cell suspensions. *D. gigas* was routinely grown on a lactate-sulfate medium as described previously (33). At the end of the exponential phase of growth, the cells were harvested by centrifugation (2,000 × *g*, 10 min) under anaerobic conditions, washed once with an oxygen-free buffer solution, and suspended in the same buffer. The cell densities of these suspensions varied between 10 and 40 mg of dry mass ml^{-1} depending on the type of experiment to be performed.

Preparation of cell extracts for determination of enzyme activities. Cell extracts were prepared from fresh cell suspensions of *D. gigas*. Cells were disrupted either by ultrasonic disintegration in an ice-cold bath or by passing the cell suspensions twice through a French pressure cell at 3.3 MPa; cell debris was removed by centrifugation (100,000 × *g*, 45 min). The composition of the buffer solutions used varied with the particular enzyme activity to be assayed. Whenever necessary, cell extracts were desalted and depleted of low-molecular-mass cofactors by passage through a Sephadex G-25 column (10 cm by 10 mm; Pharmacia Fine Chemicals) previously equilibrated with the appropriate buffer solution; samples (2.5 ml) were eluted with 3.5 ml of the same buffer.

Determination of enzyme activities. Unless otherwise stated, enzyme activities were measured spectrophotometrically at 35°C, with reaction mixtures of 1 ml total volume; the formation or the disappearance of NAD(P)H was recorded continuously at 340 nm. Ultracentrifuged and desalted cell extracts were used for these assays, unless otherwise stated; during the determinations, the cell extracts were maintained under an argon atmosphere in an ice-cold bath, and samples were withdrawn with a microsyringe through serum caps. Measurements were repeated at least three times. One milliunit (1 mU) of enzyme activity is defined as the amount catalyzing the formation of 1 nmol of product or the consumption of 1 nmol of substrate per minute.

Glycogen phosphorylase activity (EC 2.4.1.1) was assayed in the direction of glycogen phosphorolysis by coupling to phosphoglucomutase and glucose-6-phosphate dehydrogenase, as described by Khandelwal et al. (16); glycogen from rabbit liver was utilized as the substrate in this assay and was added as a homogeneous colloidal solution. The measurements were performed with undialyzed cell extracts previously treated with 20 mM $MnCl_2$ to precipitate endogenous phosphate; after incubation for 30 min at 4°C, the mixture was centrifuged at 50,000 × *g* for 30 min (42). Phosphoglucomutase (EC 5.4.2.2) was measured with undialyzed cell extracts as described by Yu et al. (42).

Glucokinase (EC 2.7.1.2), phosphoglucoisomerase (EC 5.3.1.9), phosphofructokinase (EC 2.7.1.11), fructose-1,6-bisphosphate aldolase (EC 4.1.2.13), triosephosphate isomerase (EC 5.3.1.1), enolase (EC 4.2.1.11), pyruvate kinase (EC 2.7.1.40), glucose-6-phosphate dehydrogenase (EC 1.1.1.49), and glucose dehydrogenase (EC 1.1.99.10) were measured by the methods described by Schäfer and Schönheit (34). Glyceraldehyde-3-phosphate dehydrogenase (EC 1.2.1.12) and phosphoglycerate mutase (EC 5.4.2.1) were tested by use of the assays described by Hensel et al. (12). Phosphoglycerate kinase (EC 2.7.2.3) was assayed by the method of Maitra and Lobo (21). Acetate kinase (EC 2.7.2.1), acetaldehyde dehydrogenase (EC 1.2.1.10), NAD(P)$^+$-dependent glycerol-3-phosphate dehydrogenase (EC 1.1.1.94), 6-phosphogluconate dehydrogenase (EC 1.1.1.44), and xylulose-5-phosphate phosphoketolase (EC 4.1.2.9) were measured as described by Veiga-da-Cunha et al. (41). Ethanol dehydrogenase (EC 1.1.1.1) and pyruvate decarboxylase (EC 4.1.1.1) were assayed as described by Postma et al. (29). The combined activities of 6-phosphogluconate dehydratase (EC 4.2.1.12) and 2-keto-3-deoxy-6-phosphogluconate aldolase (EC 4.1.2.14) as well as the combined activities of gluconate dehydratase and 2-keto-3-deoxygluconate aldolase were tested by the method described by Budgen and Danson (2).

NAD(P)$^+$-independent glycerol-3-phosphate dehydrogenase (EC 1.1.99.5) was assayed in the direction of glycerol-3-phosphate oxidation, as described by Kremer and Hansen (17), in MOPS buffer (50 mM MOPS potassium salt, 1 mM $MgCl_2$ [pH 7.8]), with 0.3 mM PMS plus 1.2 mM MTT or 5 mM NAD^+ as electron acceptors in the presence of 5 mM L-glycerol-3-phosphate and 10 mM NaF; this compound was included in the reaction mixture to prevent the utilization of glycerol-3-phosphate by the Embden-Meyerhof pathway. Previous studies have shown that fluoride is an effective inhibitor of enolase in *D. gigas* (33). These assays were performed with crude cell extracts (not centrifuged), desalted and depleted of low-molecular-weight cofactors as described above. The production of the reduced form of MTT was monitored at 578 nm (ε_{578} = 13 mM^{-1}). The oxidation rate of L-glycerol-3-phosphate in the presence of electron acceptors was also determined under similar conditions from the rate of disappearance of the intensity of the ^{31}P-NMR signal due to glycerol-3-phosphate.

The activity of glycerophosphatase (EC 3.1.3.1.2) was determined by measuring the formation of orthophosphate from glycerol-3-phosphate (41); orthophosphate was quantified by the method of Fiske and Subarrow (8).

Methylglyoxal synthase (EC 4.2.99.11) and glyoxalase I (EC 4.4.1.5) were tested in crude cell extracts as described by Oren and Gurevich (26) by monitoring the time course of methylglyoxal formation from dihydroxyacetone phosphate or the consumption of methylglyoxal added to the cell extracts, respectively. The reaction was started by the addition of the substrate, and after different incubation times, samples were withdrawn and assayed for methylglyoxal; methylglyoxal was determined colorimetrically with 2,4-dinitrophenylhydrazine (26). Utilization of dihydroxyacetone phosphate (or methylglyoxal) and formation of products resulting from the metabolism of these compounds were also probed by ^{1}H-NMR, with the reaction mixtures described by Oren and Gurevich (26) but with higher substrate concentrations (9 mM dihydroxyacetone phosphate for methylglyoxal synthase and 2.5 mM methylglyoxal for glyoxalase I); the reaction mixtures for both reactions contained 10 mM NaF to prevent the consumption of the substrates or the reaction products by the reactions of the Embden-Meyerhof pathway. Once the assay reaction stopped, the cell extracts were treated with HCl (70 mM final concentration) and centrifuged; the supernatant fractions were neutralized, and the low-molecular-mass compounds present were quantified by ^{1}H-NMR. Methylglyoxal dehydrogenase (EC 1.2.1.23) was assayed by the method described by Taylor et al. (39).

Lactate dehydrogenase was assayed anaerobically in desalted crude cell extracts by the method described by Stams and Hansen (36) but slightly modified: the time course for the reduction of 10 mM DCPIP was determined in the presence of 20 mM PMS, 100 mM lithium lactate, 100 mM potassium phosphate (pH 7.0), and crude cell extract corresponding to 1.6 mg of protein. Oxidized pyridine nucleotides were also tested as cofactors, and both D- and L-lactate were assayed as substrates for the reaction. The formation of the reduction product of DCPIP was monitored at 600 nm (ε_{600} = 2.1 × 10^4 M^{-1}).

^{13}C-labeling experiments with cell extracts. Cell extracts of *D. gigas* were prepared as described above by ultrasonic treatment of cell suspensions in phosphate buffer (20 mM potassium phosphate, 1 mM $MgCl_2$ [pH 7.5]). After the addition of 20 mM glucose selectively labeled with ^{13}C, the cell extracts were incubated for 6 h at 35°C under an argon atmosphere. Parallel experiments in which the assay mixture also contained 10 mM sodium fluoride were carried out. The ^{13}C-labeling pattern in acetate formed from ^{13}C-enriched glucose was determined by ^{1}H- and ^{13}C-NMR analyses of cell extracts (35). Separate experiments were performed with [1-^{13}C]glucose, [2-^{13}C]glucose, [3-^{13}C]glucose, or [6-^{13}C]glucose. Glucose utilization rates were checked by natural-abundance ^{13}C-NMR in cell extracts and in whole cell suspensions supplied with nonlabeled glucose.

Quantification of end products derived from polyglucose. Cell suspensions of *D. gigas* (approximately 15 mg of dry mass ml^{-1}) were prepared in MOPS buffer (50 mM MOPS sodium salt, 1 mM $MgCl_2$ [pH 7.8]) and transferred to Warburg flasks equipped with one side arm and a central well, previously degassed and maintained under an argon atmosphere. A volume of 300 μl of 10 N KOH was distributed between the side arm and the central cup of the flask to trap CO_2; small pieces of filter paper folded accordion style and moistened with the alkali solution were also inserted in the central well. Whenever used, solutions of the different electron acceptors (sulfate, thiosulfate, and nitrite) were added immediately before the beginning of the experiment. Cell suspensions were incubated at 35°C in the water bath attached to the Warburg respirometer, and H_2 production was measured several times for up to 2 h. At the end of the incubation time, the cell suspensions were centrifuged and the resulting supernatant solutions were analyzed by ^{1}H- and ^{13}C-NMR for identification of products. Acetate, glycerol, and ethanol were quantified enzymatically with the appropriate test combination kits from Boehringer. The effect of sodium fluoride on the pattern of end products was also examined; an identical procedure was used for these experiments except that before assays, the cells were suspended in a buffer solution containing 10 mM NaF, incubated for 20 min at room temperature, and then washed and suspended in the same NaF-containing buffer solution.

Quantification of phosphorylated metabolites. Cell suspensions (approximately 30 mg of dry mass ml^{-1}) were prepared in MOPS buffer (50 mM MOPS sodium salt, 1 mM $MgCl_2$ [pH 7.8]) as described above. The levels of NTP and phosphomonoester compounds were monitored in vivo by ^{31}P-NMR before and after the addition of 10 mM NaF to the cell suspensions. After approximately 30 min of incubation in the presence of the inhibitor, the cells were broken by ultrasonication in an ice-cold bath and proteins were precipitated by the addition of 0.5% trichloroacetic acid. These extracts were centrifuged (10,000 × *g*, 1 h); the resulting supernatant solutions were neutralized, 10 mM EDTA was added, and the samples were analyzed by ^{31}P-NMR for quantification of phosphorylated compounds.

NMR spectroscopy. NMR spectra were recorded on a Bruker AMX-500 spectrometer. ^{1}H-NMR spectra were acquired with a 5-mm selective probe head, with presaturation of the water signal; free induction decays were acquired in 16,384 data points covering a spectral width of 5 kHz, by use of a 45° flip angle and a repetition time of 6.6 s. For quantitative measurements of metabolites, 32,768 data points were collected by use of 45° pulses and a recycle delay of 23 s; the intensity of the resonance due to a known amount of formate added to the sample was used for quantification. Chemical shifts were referenced with respect to sodium 3-trimethylsilyl[2,2,3,3-^{2}H]propionate.

^{13}C-NMR spectra were obtained in a 5-mm selective probe head with proton

broadband decoupling, by use of a 45° flip angle, a 6.1-s recycle delay, 131,072 acquisition data points, and 38-kHz spectral width.

^{31}P-NMR spectra were obtained with either a 10-mm broadband probe head for whole-cell suspensions (32) or a 5-mm broadband inverse probe head for cell extracts. In both cases, spectra were acquired without proton decoupling by use of a 45° flip angle and a 0.5-s repetition time; 16,384 data points were collected over a spectral width of 20 kHz. For quantitative measurements, spectra were acquired with proton decoupling with a 30° flip angle and a repetition delay of 30 s; the intensities of the resonances observed were compared with that of the signal due to a known amount of sodium pyrophosphate added to the sample. The probe head temperature was kept at 33°C in all experiments.

Other analytical methods. Protein concentration was measured by the Bradford method (1) with bovine serum albumin as the standard. For dry cell mass determination, cells were washed with the respective buffer solution, collected by filtration in nitrate cellulose membrane filters (0.2-μm pore size), and dried at 100°C to constant mass.

RESULTS

Determination of enzyme activities. All of the enzymes of the Embden-Meyerhof pathway leading to the formation of pyruvate from glucose-6-phosphate, as well as glycogen phosphorylase and phosphoglucomutase, catalyzing, respectively, the formation of glucose-1-phosphate from glycogen and the synthesis of glucose-6-phosphate from glucose-1-phosphate, were detected in cell extracts of *D. gigas*. High levels of acetate kinase activity, catalyzing the formation of acetate from acetylphosphate, were also found. Cell extracts of *D. gigas* also catalyzed the formation of glucose-6-phosphate from glucose and ATP, showing the presence of glucokinase activity. These results are presented in Table 1. The presence of a pyruvate phosphoroclastic system in *D. gigas* is well documented (11, 23), and, therefore, the measurement of this activity was not attempted in this study.

The activities of enzymes involved in glycolytic pathways other than the Embden-Meyerhof pathway were also examined in cell extracts. Glucose-6-phosphate dehydrogenase and 6-phosphogluconate dehydrogenase, both coupled to the reduction of $NADP^+$, were detected (6 and 4 mU mg of $protein^{-1}$, respectively); xylulose-5-phosphate phosphoketolase activity was also measured (1 mU mg of $protein^{-1}$). However, the key enzymes of the Entner-Doudoroff pathway, 6-phosphogluconate dehydratase and 2-keto-3-deoxy-6-phosphogluconate aldolase, were not detected; the corresponding enzymes of the nonphosphorylated version of the same pathway (gluconate dehydratase and 2-keto-3-deoxy-gluconate aldolase) were also not found (Table 1). In contrast, enzyme activities involved in the methylglyoxal bypass (methylglyoxal synthase, glyoxalase I, and D-lactate dehydrogenase) were detected (Table 2). Methylglyoxal synthase could be detected only by ^{1}H-NMR. In these assays, the intensity of the resonance due to dihydroxyacetone phosphate, the substrate of the reaction, decreased with time, with a concomitant increase of signals assigned to the methyl groups of acetate and lactate; no other metabolic intermediates nor methylglyoxal was detected. The very low level of methylglyoxal was probably due to rapid consumption by the subsequent reaction. An upper limit for the activity of methylglyoxal synthase was calculated from the rate of dihydroxyacetone phosphate disappearance (34 nmol min^{-1} mg of $protein^{-1}$).

A brief description of the glyoxalase system is pertinent here. This system catalyzes the conversion of methylglyoxal to D-lactate via the intermediate S-D-lactoylglutathione. It comprises two enzymes, glyoxalase I and glyoxalase II. Glyoxalase I catalyzes the formation of S-D-lactoylglutathione from the hemithioacetal formed nonenzymatically from methylglyoxal and reduced glutathione. Glyoxalase II catalyzes the hydrolysis of S-D-lactoylglutathione to D-lactate and regenerates the reduced glutathione consumed in the reaction catalyzed by glyoxalase I (40).

We measured glyoxalase I activity in cell extracts of *D. gigas* both by ^{1}H-NMR and by the off-line colorimetric method for quantification of methylglyoxal, yielding identical results. In the experiments monitored by ^{1}H-NMR, the consumption of methylglyoxal, the formation and subsequent utilization of intermediate metabolites, and the production of lactate and acetate could be observed (Fig. 1). The rate of methylglyoxal utilization was used to calculate the activity shown in Table 2. This rate was not affected by the addition of reduced glutathione to the reaction mixture; this result may be explained by the high intracellular content of glutathione (1.8 nmol mg of $protein^{-1}$) present in *D. gigas* (31).

D-Lactate dehydrogenase activity could be measured in crude cell extracts only when coupled to the reduction of DCPIP-PMS under strict anaerobic conditions; high endogenous rates (3.4 nmol min^{-1} mg of $protein^{-1}$) were measured for the reduction of DCPIP in the absence of lactate. Activity was not found in the soluble fraction of cell extracts, suggesting that the enzyme is membrane associated. $NAD(P)^+$-dependent lactate dehydrogenase activity was not detected, as evaluated from the failure of lactate (either D or L forms) to reduce pyridine nucleotides.

NAD^+-dependent methylglyoxal dehydrogenase, catalyzing the direct conversion of methylglyoxal to pyruvate, was not detected.

The activities of enzymes involved in the reactions leading to the formation of ethanol and glycerol, the two major products of polyglucose metabolism other than acetate, were also examined in cell extracts. Pyruvate decarboxylase and ethanol dehydrogenase, the two enzymes involved in the formation of ethanol from pyruvate, were determined, and ethanol dehydrogenase was found to be NAD^+ specific (Table 1).

The recommended assay for glycerol-3-phosphate dehydrogenase involved the monitoring of MTT reduction, but crude cell extracts reduced MTT at a high rate even when glycerol-3-phosphate was not added. Therefore, the activity of this enzyme was confirmed by ^{31}P-NMR from the direct measurement of the consumption rate of glycerol-3-phosphate (Table 2). $NAD(P)^+$ was not a cofactor for the enzyme.

^{13}C-labeling experiments with cell extracts. The end products derived from fermentation of glucose by cell extracts were acetate, glycerol, and ethanol, the same as those produced from the catabolism of endogenous polyglucose by whole cells. The positioning of the label in the end products formed from selectively labeled glucose is given in Table 3. The label derived from [1-^{13}C]- or [6-^{13}C]glucose ended up on the methyl groups of acetate or ethanol and the methylene groups of glycerol. On the other hand, the carboxylate group of acetate, the methylene group of ethanol, and the methylene group of glycerol were labeled when [2-^{13}C]glucose was utilized. Identical labeling patterns were obtained in experiments in which 10 mM sodium fluoride was also added. Acetate or ethanol was not labeled when [3-^{13}C]glucose was provided, but glycerol was labeled on the methylene groups.

Cell suspensions of *D. gigas* utilized glucose only at very low rates (approximately 0.4 nmol min^{-1} mg of $protein^{-1}$). This may be due to inefficient transport of glucose by whole cells since glucose consumption was significantly faster in cell extracts (approximately 2 nmol of glucose min^{-1} mg of $protein^{-1}$).

End products from endogenous polyglucose. *D. gigas* cell suspensions were allowed to metabolize endogenous polyglucose under different fermentative or respiratory conditions, and the time course for hydrogen production was measured

TABLE 1. Specific activities of glycolytic and ethanol-forming enzymes in cell extracts of *D. gigas*

Enzyme	Substrate[a]	Cofactor	Sp act (mU mg of protein^{-1})[b]
Glycogen phosphorylase	Glycogen		0.7
Phosphoglucomutase	Glucose-1-phosphate		35
Glucokinase	Glucose		38
Phosphoglucoisomerase	Fructose-6-phosphate		365
Phosphofructokinase	Fructose-6-phosphate		47
Fructose 1,6-bisphosphate aldolase	Fructose-1,6-bisphosphate		5
Triosephosphate isomerase	Glyceraldehyde-3-phosphate		1,080
Glyceraldehyde-3-phosphate dehydrogenase	Glyceraldehyde-3-phosphate	NAD^+	102
	Glyceraldehyde-3-phosphate	$NADP^+$	No reaction
Phosphoglycerate kinase	3-Phosphoglycerate		142
Phosphoglycerate mutase	3-Phosphoglycerate		47
Enolase	2-Phosphoglycerate		91
Pyruvate kinase	Phosphoenolpyruvate		24
Acetate kinase	Acetate		6,085
Glucose 6-phosphate dehydrogenase	Glucose-6-phosphate	$NADP^+$	6
	Glucose-6-phosphate	NAD^+	0.1
	Glucose-6-phosphate	Methylviologen	No reaction
	Glucose-6-phosphate	Benzylviologen	No reaction
6-Phosphogluconate dehydrogenase	6-Phosphogluconate	$NADP^+$	4
	6-Phosphogluconate	NAD^+	0.2
6-Phosphogluconate dehydratase + 2-keto-3-deoxy-6-phosphogluconate aldolase	6-Phosphogluconate		No reaction
Glucose dehydrogenase	Glucose	$NADP^+$	0.1
	Glucose	NAD^+	0.1
	Glucose	Methylviologen	No reaction
	Glucose	Benzylviologen	No reaction
Gluconate dehydratase + 2-keto-3-deoxygluconate aldolase	Gluconate		No reaction
Xylulose 5-phosphate phosphoketolase	Xylulose-5-phosphate		1
Acetaldehyde dehydrogenase	Acetyl-CoA	NADH	No reaction
	Acetyl-CoA	NADPH	No reaction
Pyruvate decarboxylase	Pyruvate		10
Ethanol dehydrogenase	Acetaldehyde	NADH	3

[a] CoA, coenzyme A.
[b] Values are averages of at least three independent experiments.

over a period of 2 h. Hydrogen was formed at a constant rate of approximately 1.2 nmol min^{-1} mg of dry $mass^{-1}$. The amounts of the nongaseous carbon compounds as well as H_2 produced, determined at the end of the incubation, are shown in Table 4 and Fig. 2. In separate experiments, the time course for the production of acetate was monitored in vivo by ^1H-NMR, and a linear relationship was observed up to 2 h of incubation (rates of approximately 1 nmol of acetate min^{-1} mg of dry $mass^{-1}$, in either the absence or presence of 10 mM sodium fluoride). The energy status of the cells and the levels of inorganic phosphate were also monitored in parallel experiments by ^{31}P-NMR. The level of ATP was maintained at approximately 3 to 4 mM for at least 3 h, and the pool of inorganic phosphate was always higher than that of ATP. Under fermentative conditions, high levels of glycerol, ethanol, and H_2 were produced in addition to acetate (Fig. 2). When the results in the presence and absence of fluoride are compared, the major differences are the higher production of H_2 and the lower molar ratio of glycerol/acetate in the absence of the inhibitor. It is also relevant that equimolar amounts of

TABLE 2. Specific activities in cell extracts of *D. gigas* of enzymes of the methylglyoxal bypass or involved in glycerol-forming reactions

Enzyme	Substrate	Cofactor	Sp act (mU mg of protein^{-1})[a]
Methylglyoxal synthase	Dihydroxyacetone phosphate		2–34
Glyoxalase I	Methylglyoxal		35
Lactate dehydrogenase	D-Lactate	MTT-PMS	0.68
	L-Lactate	MTT-PMS	2.18
	D- or L-lactate	NAD^+	No reaction
Methylglyoxal dehydrogenase	Methylglyoxal	NAD^+	No reaction
Glycerol-3-phosphate dehydrogenase	Glycerol-3-phosphate	MTT-PMS	4
	Glycerol-3-phosphate	NAD^+	No reaction
	Glycerol-3-phosphate	$NADP^+$	No reaction
Glycerol phosphatase	Glycerol-3-phosphate		4

[a] Values are averages of at least three independent experiments.

acetate, glycerol, and molecular hydrogen were formed by cells treated with NaF. In contrast, when an electron acceptor was provided, acetate was the major nongaseous carbon product formed, H_2, glycerol, and ethanol being either absent or present in vestigial amounts (Fig. 2).

It will become apparent in our discussion below that the reaction leading to the formation of ethanol uses NADH that can be formed only in the reaction catalyzed by glyceraldehyde-3-phosphate dehydrogenase; since fluoride is known to be an inhibitor of enolase in this organism (33), the formation of ethanol (40 nmol mg of dry mass^{-1}) (Table 4) by cells treated with fluoride cannot be immediately explained. To elucidate this question, cell suspensions were incubated for 30 min in the presence of sodium fluoride and the phosphorylated metabolites accumulated intracellularly were quantified in the corresponding cell extracts: 25 nmol of 3-phosphoglycerate per mg of dry mass and 5 nmol of glycerol-3-phosphate per mg of dry mass were determined.

DISCUSSION

Our early work on polyglucose utilization by *D. gigas* suggested the existence of two different glycolytic pathways for the

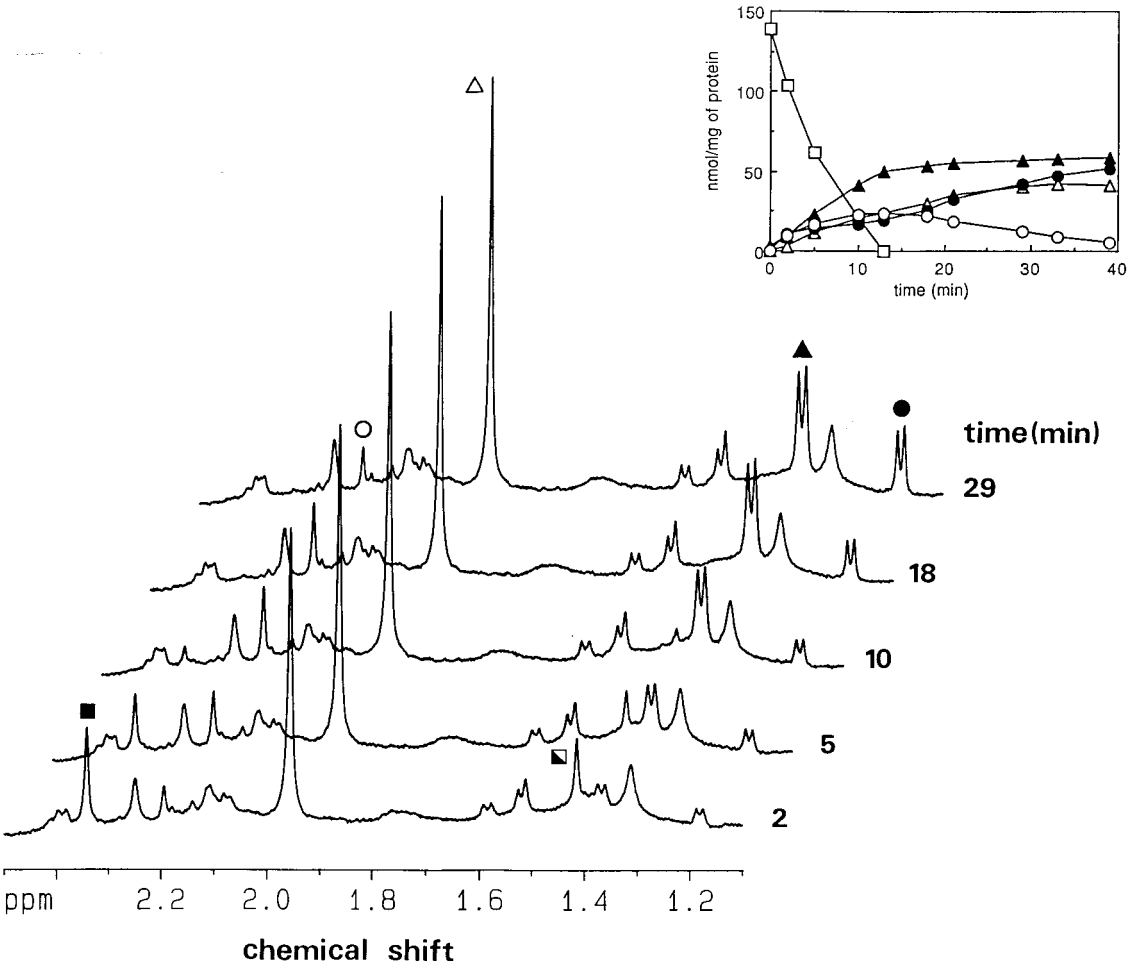

FIG. 1. Glyoxalase I activity in cell extracts of *D. gigas* monitored by ^{1}H-NMR; the time course for the consumption of methylglyoxal and the production of lactate and acetate are shown. The reaction mixture was prepared in 50 mM potassium phosphate buffer (pH 6.8) containing 10 mM NaF, 2.5 mM methylglyoxal, and 14 mg of protein in a total volume of 0.75 ml. Inset, plot of the concentrations of several metabolites as a function of time after the addition of methylglyoxal. The amount of acetate in the initial preparation before the addition of methylglyoxal was subtracted. Symbols: ■, methylglyoxal; ◪, methylglyoxal hydrate; □, methylglyoxal plus hydrate; △, acetate; ▲, lactate; ● and ○, intermediate metabolites tentatively assigned to *S*-D-lactoylglutathione and hemithioacetal, respectively.

TABLE 3. Labeling pattern of the end products formed by cell extracts of *D. gigas* from glucose selectively enriched with ^{13}C[a]

Substrate	Labeing of end products					
	Acetate		Glycerol		Ethanol	
	C_1	C_2	C_1 or C_3	C_2	C_1	C_2
[1-^{13}C]glucose	−	+	+	−	−	+
[1-^{13}C]glucose + NaF	−	+	+	−	−	+
[2-^{13}C]glucose	+	−	−	+	+	−
[2-^{13}C]glucose + NaF	+	−	−	+	+	−
[3-^{13}C]glucose + NaF	−	−	+	−	−	−
[6-^{13}C]glucose	−	+	+	−	−	+
[6-^{13}C]glucose + NaF	−	+	+	−	−	+

[a] Cell extracts were prepared in 20 mM potassium phosphate buffer containing 1 mM $MgCl_2$ (pH 7.8) and incubated at 35°C for 6 h after the addition of 20 mM labeled glucose. Sodium fluoride was added at a concentration of 10 mM. Data were obtained from ^{1}H- and ^{13}C-NMR analysis of the samples.

TABLE 4. End products from polyglucose utilization by cell suspensions of *D. gigas* in fermentative or respiratory conditions[a]

Incubation conditions	Amt of end product[b] (nmol mg of dry mass^{-1} [mean ± SD])			
	Acetate	Glycerol	Ethanol	H_2
Without additions	84 ± 9	38 ± 9	79 ± 6	140 ± 11
With 10 mM NaF	85 ± 8	89 ± 5	40 ± 2	69 ± 10
With 20 mM sodium nitrite	145 ± 11	4 ± 0.5	0	0
With 20 mM sodium thiosulfate	155 ± 8	4 ± 0.5	0	0
With 20 mM sodium sulfate	202 ± 10	0	0	0

[a] Cell suspensions were prepared in 50 mM MOPS buffer containing 1 mM $MgCl_2$ (pH 7.8) and incubated under an argon atmosphere at 35°C for 2 h. The effects of sodium fluoride and different electron acceptors (sodium nitrite, sodium thiosulfate, and sodium sulfate) were probed. End products were quantified as described in Materials and Methods.

[b] The data presented correspond to the average of the values obtained in two similar experiments (two replicates in each experiment), except for row 1 of data, where four independent experiments were performed.

oxidation of glucose-6-phosphate to acetate, one involving enolase and another excluding the participation of this enzyme (33). In regard to the nature of the glycolytic pathways that convert glucose to pyruvate and involve enolase, several hypotheses were considered, namely, the Embden-Meyerhof pathway, the Entner-Doudoroff pathway, the pentose phosphate pathway, and the heterofermentative pathway. Determinations of enzyme activities in cell extracts of *D. gigas* ruled out the presence of both phosphorylated and nonphosphorylated versions of the Entner-Doudoroff pathway, since 6-phosphogluconate dehydratase, 2-keto-3-deoxy-6-phosphogluconate aldolase, and the corresponding enzymes of the nonphosphorylated pathway could not be detected. In contrast, all of the activities of the Embden-Meyerhof pathway were observed as well as those catalyzing the steps leading to the formation of glycerol and ethanol. These findings are consistent with the data obtained from experiments with selectively labeled [^{13}C]glucose which support the operation of the Embden-Meyerhof pathway for the catabolism of polyglucose. Although the activities of glucose-6-phosphate dehydrogenase, 6-phosphogluconate dehydrogenase, and xylulose-5-phosphate phosphoketolase were present, analysis of the labeling pattern of the end products derived from utilization of [^{13}C]glucose ruled out the involvement of either the pentose phosphate pathway or the heterofermentative pathway. If either of these pathways (or both) would be operating, the label from [2-^{13}C]glucose would end up on the methyl group of acetate and not on the carboxylate group, as was observed.

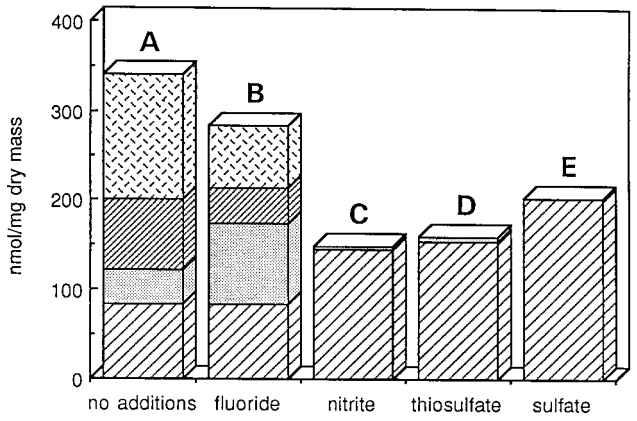

FIG. 2. End products derived from polyglucose utilization by cell suspensions of *D. gigas* under fermentative conditions (A and B) or in the presence of nitrite (C), thiosulfate (D), or sulfate (E). The data correspond to the values shown in Table 4. Symbols: ⊘, acetate; ▤, glycerol; ▨, ethanol; ▩, molecular hydrogen.

The activities of the glycolytic enzymes involved in the conversion of dihydroxyacetone phosphate to pyruvate and of NAD^+-dependent ethanol and acetaldehyde dehydrogenases were previously detected in cell extracts of lactate-grown *D. gigas* (17, 18), but phosphofructokinase, the key enzyme of the Embden-Meyerhof pathway, is reported here for the first time. The presence of a pyridine nucleotide-independent glycerol-3-phosphate dehydrogenase is in line with early data by Kremer and Hansen (17) for *Desulfovibrio vulgaris* and two marine strains of *Desulfovibrio* grown on lactate-sulfate medium and for *D. gigas* grown on glycerol. These authors were unable to detect this activity in cell extracts of *D. gigas* grown on lactate-sulfate; we were able to measure this enzyme, but only a low activity was found.

The data presented here show that in addition to using the Embden-Meyerhof pathway, *D. gigas* uses the methylglyoxal bypass for the conversion of triose phosphate to acetate. The methylglyoxal bypass is present in different types of microorganisms such as bacteria, archaebacteria, and yeast (9, 15). It has been suggested that the methylglyoxal bypass provides an alternative catabolic route for triose phosphates formed during glycolysis because the methylglyoxal synthase of *Escherichia coli* is inhibited by concentrations of inorganic phosphate similar to the K_m value for this ion of glyceraldehyde-3-phosphate dehydrogenase (13, 14). However, this rationale is not applicable to yeast, in which the methylglyoxal synthase activity was found to be relatively insensitive to the level of inorganic phosphate (22); this seems to be the case in *D. gigas* as well since the methylglyoxal pathway is operating despite the high intracellular levels of inorganic phosphate detected by in vivo ^{31}P-NMR.

The labeling pattern of the end products obtained from the catabolism of [^{13}C]glucose when the Embden-Meyerhof pathway is inhibited at the level of enolase agrees with the operation of the methylglyoxal bypass. Moreover, two key enzymes of this pathway, methylglyoxal synthase and glyoxalase I, were detected in crude cell extracts of *D. gigas*, and the values determined for the activities were consistent with the rates of acetate production from polyglucose observed in whole cells treated with fluoride (approximately 1 nmol min^{-1} mg of dry mass^{-1}). The activities measured for methylglyoxal synthase

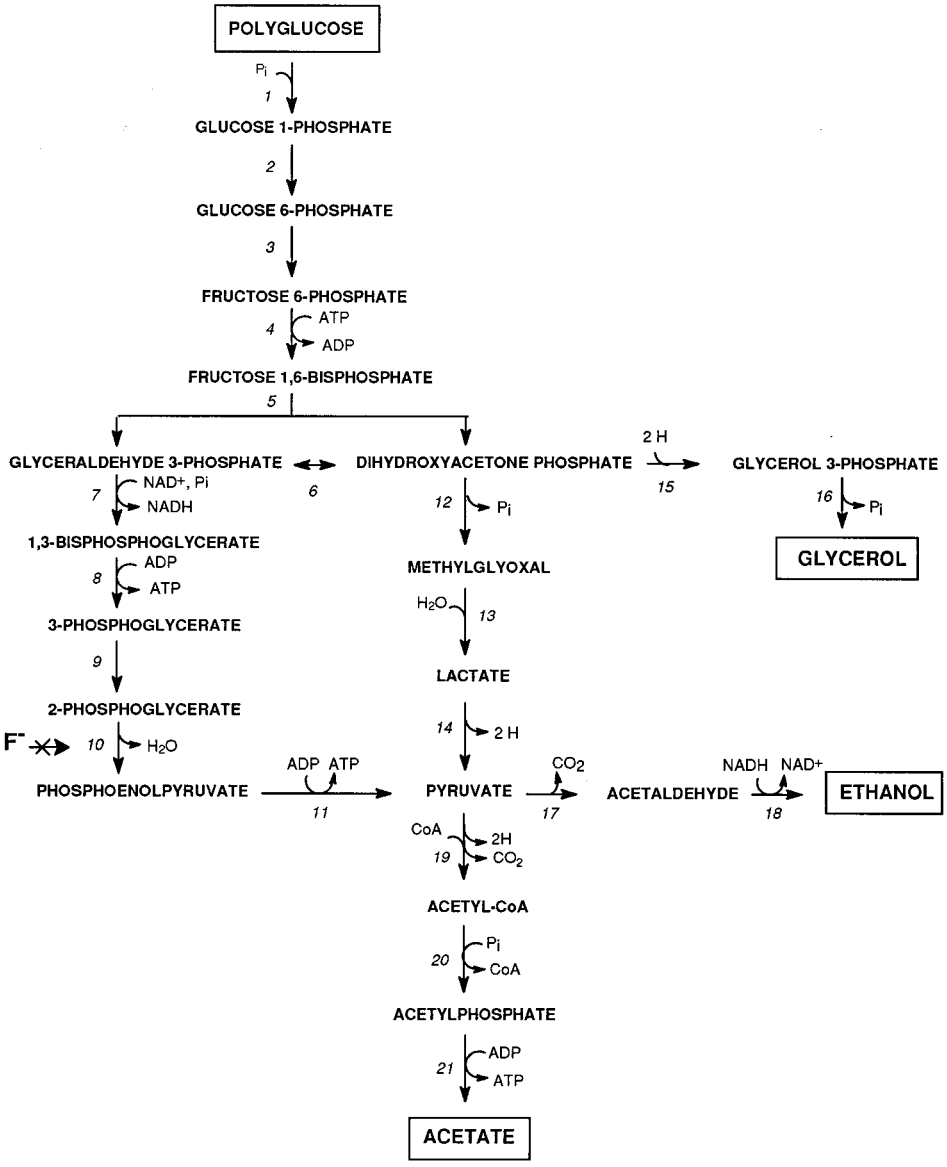

FIG. 3. Proposed metabolic pathways for polyglucose utilization by *D. gigas*. The numbers designate the enzymes catalyzing the corresponding reactions: *1*, polyglucose phosphorylase; *2*, phosphoglucomutase; *3*, phosphoglucoisomerase; *4*, phosphofructokinase; *5*, fructose-1,6-bisphosphate aldolase; *6*, triosephosphate isomerase; *7*, glyceraldehyde-3-phosphate dehydrogenase; *8*, 3-phosphoglycerate kinase; *9*, phosphoglycerate mutase; *10*, enolase; *11*, pyruvate kinase; *12*, methylglyoxal synthase; *13*, glyoxalase I and II; *14*, lactate dehydrogenase; *15*, glycerol-3-phosphate dehydrogenase; *16*, glycerophosphatase; *17*, pyruvate decarboxylase; *18*, ethanol dehydrogenase; *19*, pyruvate:ferredoxin oxidoreductase; *20*, phosphotransacetylase; *21*, acetate kinase.

and glyoxalase I in *D. gigas* are comparable to those reported for other organisms such as *Saccharomyces cerevisiae* (27), *Pseudomonas saccharophila* (5), and halophilic archaebacteria (26). D-Lactate dehydrogenase, the enzyme that catalyzes the conversion of D-lactate to pyruvate, was also detected in *D. gigas* (this work), and this activity was membrane linked and pyridine nucleotide independent, the natural electron acceptors for the reaction remaining unknown. The presence of pyridine nucleotide-independent D-lactate dehydrogenase activity has been also reported in the soluble and membrane fractions of several strains of *Desulfovibrio* (6, 24, 36).

The data presented in this work support the metabolic scheme proposed in Fig. 3 for polyglucose utilization by *D. gigas*. According to this proposal, the operation of the Embden-Meyerhof pathway for the catabolism of polyglucose leads to the production of NADH at the level of glyceraldehyde-3-phosphate dehydrogenase. At least part of the NAD^+ consumed for the oxidation of glyceraldehyde-3-phosphate is regenerated by the reaction catalyzed by ethanol dehydrogenase, which is also a pyridine nucleotide-dependent enzyme. The reducing equivalents derived from the glyceraldehyde-3-phosphate dehydrogenase step are not expected to be used for the production of glycerol, since glycerol-3-phosphate dehydrogenase was shown to be NADH independent. It is expected that the combined activities of pyruvate:ferredoxin oxidoreductase and hydrogenase lead to the production of equimolar amounts of acetyl-coenzyme A and molecular hydrogen (28), but in the catabolism of polyglucose by whole cells, an excess of 60 nmol of H_2 per mg of dry mass over acetate was produced (Table 4, row 1). This result suggests that at least some of the reducing equivalents derived

from NADH were consumed for the production of molecular hydrogen. Moreover, when enolase was inhibited, and therefore the methylglyoxal bypass was operating alone, equimolar amounts of acetate, glycerol, and molecular hydrogen were produced (Table 4, row 2). This shows that the reducing equivalents derived from the oxidation of D-lactate to pyruvate were channeled to the reduction of dihydroxyacetone phosphate to glycerol-3-phosphate. Therefore, we conclude that the extra reducing equivalents used for the production of molecular hydrogen in untreated cells were derived from the fraction of the NADH formed by glyceraldehyde-3-phosphate dehydrogenase which was not consumed by ethanol dehydrogenase.

The relative contributions of the Embden-Meyerhof pathway and the methylglyoxal bypass for the catabolism of polyglucose in *D. gigas* under fermentative conditions is easily estimated from the amounts of end products shown in Table 4. Since the amount of glycerol produced is a direct measure of the substrate flow via the methylglyoxal bypass, it is concluded that 38 nmol of glucose per mg of dry mass was converted through the methylglyoxal bypass, whereas $(79 + 84 - 38)/2$ nmol of glucose per mg of dry mass was catabolized by the Embden-Meyerhof pathway. In conclusion, approximately 40% of glucose residues were degraded via the methylglyoxal bypass, whereas the remaining 60% were converted via the Embden-Meyerhof pathway. The determination of the full mass balance, including the quantification of polyglucose utilization, would provide further support for the metabolic scheme proposed in this study. The methylglyoxal bypass has been found in a wide variety of organisms, but its physiological role is not well understood (15). The relatively high contribution of the methylglyoxal pathway in the fermentation of polyglucose in *D. gigas* is difficult to rationalize on the basis of the data presently available; according to the scheme shown in Fig. 3, 5 mol of ATP can be conserved for each glucose residue that is catabolized via the Embden-Meyerhof pathway, whereas no net ATP synthesis occurs if polyglucose is degraded in the methylglyoxal shunt. Therefore, the operation of this pathway under fermentative conditions results in uncoupling of substrate utilization and ATP production.

The significant amounts of ethanol produced by cells treated with fluoride are not readily explained. However, despite the inhibition of enolase, it is conceivable that an equivalent amount of NADH could be formed by glyceraldehyde-3-phosphate dehydrogenase, leading to the accumulation of phosphorylated glycolytic metabolites. The NADH produced in this way would then be used to form ethanol from pyruvate. In fact, this hypothesis is supported by the level of 3-phosphoglycerate determined in cells treated with fluoride (25 nmol mg of dry mass^{-1}), which is of the same order of magnitude as the amount of ethanol produced (40 nmol mg of dry mass^{-1}).

When *D. gigas* was allowed to catabolize polyglucose in the presence of an electron acceptor (nitrite, thiosulfate, or sulfate), acetate was by far the major end product, showing that reducing equivalents originating from glucose oxidation were used to reduce the terminal electron acceptors. Furthermore, the lack of ethanol and net amounts of hydrogen in the end products also confirms that NADH originating from glyceraldehyde-3-phosphate dehydrogenase must be oxidized by the final electron acceptor, via either H_2 or another yet-unknown pathway. By allowing an efficient removal of hydrogen, the presence of an electron acceptor could make thermodynamically favorable the otherwise unfavorable process of transferring reducing equivalents from NADH to H^+. However, this study does not permit us to discriminate between this hypothesis and another, in which hydrogen recycling would not be invoked.

Several reports are available in the literature indicating that in *Desulfovibrio*, NAD(P)H can act as a redox carrier during the catabolism of various substrates, such as ethanol, C_4-dicarboxylic acids, glycerol, and amino acids (3, 17, 18, 20, 37). Moreover, NADH oxidation coupled to the reduction of APS, thiosulfate, or fumarate was demonstrated in a marine strain of *Desulfovibrio* (19). More recently, an NADH dehydrogenase was isolated from *D. vulgaris* with the ability to fully reduce APS reductase was isolated from *D. vulgaris* from the same organism (4). Together with these observations, our results reinforce the view that NADH can play an important role in the overall metabolism of *Desulfovibrio*, linking substrate oxidation to the reduction of terminal electron acceptors.

ACKNOWLEDGMENTS

We thank T. Hansen for helpful discussions.

This work was supported by PRAXIS XXI and FEDER, Lisbon, Portugal (PRAXIS/2/2.1/BIO/20/94).

REFERENCES

1. **Bradford, M. M.** 1976. A rapid and sensitive method for the quantitation of microgram quantities of protein utilizing the principle of protein dye binding. Anal. Biochem. **72:**248–254.
2. **Budgen, N., and M. J. Danson.** 1986. Metabolism of glucose via a modified Entner-Doudoroff pathway in the thermoacidophilic archaebacterium *Thermoplasma acidophilum*. FEBS Lett. **196:**207–210.
3. **Chen, L., J. LeGall, P. Fareleira, H. Santos, and A. V. Xavier.** 1995. Malate metabolism by *Desulfovibrio gigas* and its link to sulfate and fumarate reduction: purification of the malic enzyme and detection of NAD(P)$^+$ transhydrogenase activity. Anaerobe **1:**227–235.
4. **Chen, L., J. LeGall, and A. V. Xavier.** 1994. Purification, characterization and properties of an NADH oxidase from *Desulfovibrio vulgaris* (Hildenborough) and its coupling to adenylyl phosphosulfate reductase. Biochem. Biophys. Res. Commun. **203:**839–844.
5. **Cooper, R. A.** 1974. Methylglyoxal formation during glucose catabolism by *Pseudomonas saccharophila*. Eur. J. Biochem. **44:**81–86.
6. **Czechowski, M. H., and H. W. Rossmore.** 1980. Factors affecting *Desulfovibrio desulfuricans* lactate dehydrogenase. Dev. Ind. Microbiol. **21:**349–356.
7. **Dawes, E. A., and P. J. Senior.** 1973. The role and regulation of energy reserve polymers in micro-organisms. Adv. Microb. Physiol. **10:**135–266.
8. **Fiske, C. H., and Y. P. Subarrow.** 1925. The colorimetric determination of phosphorus. J. Biol. Chem. **66:**375–400.
9. **Gottschalk, G.** 1986. Bacterial metabolism, 2nd ed. Springer-Verlag, New York, N.Y.
10. **Hansen, T. A.** 1993. Carbon metabolism of sulfate-reducing bacteria, p. 21–40. *In* J. M. Odom and R. Singleton, Jr.(ed.), The sulfate reducing bacteria: contemporary perspectives. Springer, Verlag, New York, N.Y.
11. **Hatchikian, E. C., and J. LeGall.** 1970. Étude du métabolisme des acides dicarboxyliques et du pyruvate chez les bactéries sulfato-réductrices. I. Étude de lóxydation enzymatic du fumarate en acétate. Ann. Inst. Pasteur **188:**125–142.
12. **Hensel, R., S. Laumman, J. Lang, H. Heumann, and F. Lottspeich.** 1987. Characterization of two D-glyceraldehyde 3-phosphate dehydrogenases from the extremely thermophilic archaebacterium *Thermoproteus tenax*. Eur. J. Biochem. **170:**325–333.
13. **Hopper, D. J., and R. A. Cooper.** 1972. Purification and properties of *Escherichia coli* methylglyoxal synthase. Biochem. J. **128:**321–329.
14. **Hopper, D. J., and R. A. Cooper.** 1971. The regulation of *Escherichia coli* methylglyoxal sinthase; a new control site in glycolysis? FEBS Lett. **13:**213–216.
15. **Inoue, Y., and A. Kimura.** 1995. Methylglyoxal and regulation of its metabolism in microorganisms. Adv. Microb. Physiol. **37:**177–227.
16. **Khandelwal, R. L., T. N. Spearmen, and I. R. Hamilton.** 1973. Purification and properties of glycogen phosphorylase from Streptococcus salivarius. Arch. Biochem. Biophys. **154:**295–305.
17. **Kremer, D. R., and T. A. Hansen.** 1987. Glycerol and dihydroxyacetone phosphate dissimilation in *Desulfovibrio* strains. Arch. Microbiol. **147:**249–256.
18. **Kremer, D. R., H. E. Nienhuis-Kuiper, and T. A. Hansen.** 1988. Ethanol dissimilation in *Desulfovibrio*. Arch. Microbiol. **150:**552–557.
19. **Kremer, D. R., and T. A. Hansen.** 1989. Demonstration of HOQNO and antimycin A sensitive coupling of NADH oxidation and APS and sulfite reduction in a marine strain of *Desulfovibrio*. FEMS Microbiol. Lett. **49:**273–277.
20. **Kremer, D. R., H. E. Nienhuis-Kuiper, C. J. Timmer, and T. A. Hansen.** 1989. Catabolism of malate and related dicarboxylic acids in various *Desulfovibrio* strains and the involvement of an oxygen-labile NADPH dehydrogenase. Arch. Microbiol. **151:**34–39.

21. **Maitra, P. K., and Z. Lobo.** 1971. A kinetic study of glycolytic enzyme synthesis in yeast. J. Biol. Chem. **246:**475–488.
22. **Murata, K., Y. Fukuda, K. Watanable, T. Saikusa, M. Shimosaka, and A. Kimura.** 1985. Characterization of methylglyoxal synthase in *Saccharomyces cerevisiae*. Biochem. Biophys. Res. Commun. **131:**190–198.
23. **Odom, J. M., and H. D. Peck, Jr.** 1981. Localization of dehydrogenases, reductases, and electron transfer components in the sulfate-reducing bacterium *Desulfovibrio gigas*. J. Bacteriol. **147:**161–169.
24. **Ogata, M., K. Arihara, and T. Yagi.** 1981. D-Lactate dehydrogenase of *Desulfovibrio vulgaris*. J. Biochem. (Tokyo) **89:**1423–1431.
25. **Ollivier, B., R. Cord-Ruwisch, E. C. Hatchikian, and J. L. Garcia.** 1988. Characterization of *Desulfovibrio fructosovorans* sp. nov. Arch. Microbiol. **149:**447–450.
26. **Oren, A., and P. Gurevich.** 1995. Occurrence of the methylglyoxal bypass in halophilic Archaea. FEMS Microbiol Lett. **125:**83–88.
27. **Penninckx, M. J., C. J. Jaspers, and M. J. Legrain.** 1983. The glutathione-dependent glyoxalase pathway in the yeast *Saccharomyces cerevisiae*. J. Biol. Chem. **258:**6030–6036.
28. **Postgate, J. R.** 1984. The sulfate-reducing bacteria. Cambridge University Press, Cambridge, United Kingdom.
29. **Postma, E., C. Verduyn, A. Scheffers, and J. P. Van Dijken.** 1989. Enzyme analysis of the cabtree effect in glucose-limited chemostat cultures of *Saccharomyces cerevisiae*. Appl. Environ. Microbiol. **55:**468–477.
30. **Preiss, J.** 1984. Bacterial glycogen synthesis and its regulation. Annu. Rev. Microbiol. **38:**419–458.
31. **Santos, B., P. Fareleira, P. Moradas-Ferreira, J. LeGall, A. V. Xavier, and H. Santos.** Unpublished data.
32. **Santos, H., P. Fareleira, J. LeGall, and A. V. Xavier.** 1994. *In vivo* nuclear magnetic resonance in study of physiology of sulfate-reducing bacteria. Methods Enzymol. **243:**543–558.
33. **Santos, H., P. Fareleira, A. V. Xavier, L. Chen, M.-Y. Liu, and J. LeGall.** 1993. Aerobic metabolism of carbon reserves by the "obligate anaerobe" *Desulfovibrio gigas*. Biochem. Biophys. Res. Commun. **195:**551–557.
34. **Schäfer, T., and P. Schönheit.** 1992. Maltose fermentation to acetate, CO_2 and H_2 in the anaerobic hyperthermophilic archaeon *Pyrococcus furiosus*: evidence for the operation of a novel sugar fermentation pathway. Arch. Microbiol. **158:**188–202.
35. **Schäfer, T., K. B. Xavier, H. Santos, and P. Schönheit.** 1994. Glucose fermentation to acetate and alanine in resting cell suspensions of *Pyrococcus furiosus*: proposal of a novel glycolytic pathway based on ^{13}C labelling data and enzyme activities. FEMS Microbiol. Lett. **121:**107–114.
36. **Stams, A. J. M., and T. A. Hansen.** 1982. Oxygen-labile L(+)lactate dehydrogenase activity in *Desulfovibrio desulfuricans*. FEMS Microbiol. Lett. **13:**389–394.
37. **Stams, A. J. M., and T. A. Hansen.** 1986. Metabolism of L-alanine in *Desulfotomaculum ruminis* and two marine *Desulfovibrio* strains. Arch. Microbiol. **145:**277–279.
38. **Stams, F. J. M., M. Veenhuis, G. H. Weenk, and T. A. Hansen.** 1983. Occurrence of polyglucose as a storage polymer in *Desulfovibrio* species and *Desulfobulbus propionicus*. Arch. Microbiol. **136:**54–59.
39. **Taylor, D. G., P. W. Trudgill, R. E. Cripps, and P. R. Harris.** 1980. The microbial metabolism of acetone. J. Gen. Microbiol. **118:**159–170.
40. **Thornalley, P. J.** 1990. The glyoxalase system: new developments towards functional characterization of a metabolic pathway fundamental to biological life. Biochem. J. **269:**1–11.
41. **Veiga-da-Cunha, M., H. Santos, and E. Van Schaftingen.** 1993. Pathway and regulation of erythritol biosynthesis in *Leuconostoc oenos*. J. Bacteriol. **175:**3941–3948.
42. **Yu, J.-P., J. Ladapo, and W. B. Whitman.** 1994. Pathway of glycogen metabolism in *Methanococcus maripaludis*. J. Bacteriol. **176:**325–332.
43. **Zellner, G., P. Messner, H. Kneifel, and J. Winter.** 1989. *Desulfovibrio simplex* spec. nov., a new sulfate-reducing bacterium from a sour whey digester. Arch. Microbiol. **152:**329–334.